# Large-Angle $\pi^-+p$ Elastic Scattering at 3.63 GeV/$c$*

MARTIN L. PERL
*Stanford Linear Accelerator Center, Stanford University, Stanford, California*

AND

YONG YUNG LEE† AND ERWIN MARQUIT
*University of Michigan, Ann Arbor, Michigan*

(Received 30 November 1964)

The differential cross section for elastic scattering of 3.63-GeV/$c$ $\pi^-$ mesons on protons was studied with a hydrogen bubble chamber, the emphasis being on large-angle scattering. From 90 to 180° in the barycentric system, the cross section is roughly flat with an average value of $2.7\pm1.0$ $\mu$b/sr. Near and at 180°, there may be a slight peak of magnitude $10\pm6$ $\mu$b/sr. But if such a peak exists, it is only one-third to one-fourth the size of the 180° peak found in 4.0 GeV/$c$ $\pi^+ + p$ elastic scattering. In addition to comparison with other $\pi^- + p$ and $\pi^+ + p$ large-angle elastic-scattering measurements, this measurement is compared with large-angle $p+p$ elastic scattering. In the forward hemisphere a small peak or a plateau exists at $\cos\theta^* = +0.60$. This appears to be a second diffraction maximum such as has been found in lower-energy $\pi+p$ elastic scattering. A survey of indications of such a second diffraction maximum in other $\pi+p$ measurements shows that it always occurs in the vicinity of $-t=1.2$ (GeV/$c$)$^2$, where $t$ is the square of the four-momentum transfer. As the incident momentum increases, the relative size of this second maximum decreases.

## I. INTRODUCTION

THIS paper describes a new bubble chamber measurement of the large-angle elastic scattering of 3.63-GeV/$c$ $\pi^-$ mesons on protons. The exposure was made in the Brookhaven National Laboratory 20-in. hydrogen bubble chamber at the AGS. In the last few years there have been several fairly precise measurements of high-energy $\pi+p$ elastic scattering in the diffraction region.[1–6] But above 2 GeV/$c$ the measurements outside the diffraction region have been poor and sometimes consist only of upper limits. This is simply because the large-angle scattering is so much smaller than the diffraction scattering. In this paper we define the large-angle scattering region as that in which the magnitude of the square of the four-momentum transfer is greater than 1 (GeV/$c$)$^2$, which means that the differential cross section has decreased by at least a factor of 100 from its 0° value.

Several years ago, Perl, Jones, and Ting[4] summarized the situation with respect to both fundamental and phenomenological theories of elastic scattering. Since that time there has been no progress in fundamental theories of the sort that would allow the present measurements to be interpreted or understood in a basic way. Neither is there a new fundamental theory to be tested by these data. There have been some refinements in the phenomenological theories, particularly with reference to large-angle scattering theories. Krisch,[7] Serber,[8] and Perl and Corey[9] have extended the optical model to large angles. Jones[10] and Woo[11] have examined further the statistical model explanation of large-angle scattering. But the theory of elastic scattering remains a puzzle, and the large-angle scattering is perhaps the hardest part of that puzzle. One very interesting fact in the large-angle scattering part of this puzzle is that the long-sought backward peak in $\pi^+ + p$ elastic scattering has been found[6] at 4 GeV/$c$. Published measurements of the $\pi^- + p$ backward elastic scattering in that momentum range are not sufficiently precise to provide a good comparison.[4,6] Therefore, one special purpose of this paper is to provide a better $\pi^- + p$ measurement for that comparison. As an aid in that comparison the analysis of Perl and Corey[9] will be used. A second special purpose is to compare large-angle $\pi^- + p$ and $p+p$ elastic scattering. The $p+p$ large-angle elastic-scattering cross section decreases very rapidly as the incident momentum and four-momentum transfer increase.[12] The question is whether the $\pi+p$ cross section also decreases as rapidly.

Beyond that we shall consider that we have added another piece of data to the experimental knowledge of elastic scattering, and we must wait patiently for a new basic theory to make use of it.

The exposure consisting of 60 000 pictures has already been described,[13] as well as the method of scanning and

* Supported in part by the U. S. Atomic Energy Commission.
† Present Address, Physics Department, University of Wisconsin, Madison, Wisconsin.
[1] D. O. Caldwell, B. Elsner, D. Harting, A. C. Helmholz *et al.*, Phys. Letters **8**, 288 (1964).
[2] K. J. Foley, S. J. Lindenbaum, W. A. Love, S. Ozaki, J. J. Russell, and L. C. L. Yuan, Phys. Rev. Letters **10**, 376 (1963).
[3] S. Brandt, V. T. Cocconi, D. R. O. Morrison, A. Wroblewski *et al.*, Phys. Rev. Letters **10**, 413 (1963).
[4] M. L. Perl, L. W. Jones, and C. C. Ting, Phys. Rev. **132**, 1252 (1963).
[5] D. E. Damouth, L. W. Jones, and M. L. Perl, Phys. Rev. Letters **11**, 287 (1963).
[6] M. Aderholz, L. Bondar, M. Deutschmann, H. Lengeler *et al.*, Phys. Letters **10**, 245 (1964); Nuovo Cimento **31**, 729 (1964).
[7] A. D. Krisch, Phys. Rev. Letters **11**, 217 (1963).
[8] R. Serber, Rev. Mod. Phys. **36**, 649 (1964).
[9] M. L. Perl and M. C. Corey, Phys. Rev. **136**, B787 (1964).
[10] L. W. Jones, Phys. Letters **8**, 287 (1964).
[11] C. H. Woo, Phys. Rev. **137**, B449 (1965).
[12] G. Cocconi, V. T. Cocconi, A. D. Krisch, J. Orear *et al.*, Phys. Rev. Letters **11**, 499 (1963).
[13] Y. Y. Lee, Technical Report, Department of Physics, University of Michigan, 1964 (unpublished).

measurement. The principal purpose of the exposure, the study of resonances, has also been described.[14] This paper describes only the elastic-scattering measurement.

## II. METHOD OF ANALYSIS AND RESULTS

Bubble chamber measurement of elastic scattering may have difficulties in both the large-angle and very small-angle region. At large angles there may be an ambiguity in that the event fits both the elastic hypothesis $\pi^-+p\rightarrow\pi^-+p$ and the one-$\pi^0$ inelastic hypothesis $\pi^-+p\rightarrow\pi^-+p+\pi^0$. At small angles, when this occurs, the bubble density of the recoil proton can usually be used to resolve this ambiguity. But this may not be possible at large angles where the recoil proton has a value of $\beta$ close to 1.

In this analysis a hypothesis was accepted if the $\chi^2$ probability was greater than 2%, and if the bubble density agreed with the proton ionization required by the hypothesis; 1218 events were found which fit only the elastic hypothesis. However, 565 more events fit both the elastic hypothesis and the one-$\pi^0$ inelastic hypothesis. These are called ambiguous elastic events. As the barycentric scattering angle of the pion increased, the proportion of ambiguous events also increased. A study of the $\chi^2$ distributions showed that the errors used in the analysis programs were approximately correct. Therefore the ambiguities were not due to too large error estimates. The simple fact is that a 20-in. bubble chamber does not provide sufficiently good momentum measurements at this momentum (3.6 GeV/$c$) to give the kind of two-prong event identification we ideally need. At the lower momentum of 3.0 GeV/$c$, Hagopian,[15] using the same chamber with similar error estimates, had little difficulty with these ambiguous elastic events. Therefore, somewhere between 3.0 and 3.6 GeV/$c$ is the threshold at which the ambiguity in the elastic event analysis in this chamber begins to appear.

The ratio of ambiguous elastic events to the sum of ambiguous and unambiguous elastic events was 0.32, but for backward barycentric scattering angles all the elastic events were ambiguous. However, we are able to show that there is only a very small contamination of inelastic events in these 565 ambiguous events and specifically that the inelastic contamination in backward angular region is less than 12.5%. This was done as follows. In this same exposure 1056 unambiguous, one-$\pi^0$ inelastic events were found. The question is: Are there sufficiently large fluctuations in the measurements of these one-$\pi^0$ inelastic events so that some of them could fit the elastic hypothesis? Each unambiguous $\pi^0$ inelastic event was regarded as an elastic event, the barycentric scattering angle being taken as the average of that given by the outgoing $\pi^-$ and that given by the outgoing proton. This angle is called the artificial elastic scattering angle. The analysis program had already calculated the $\chi^2$ value if that inelastic event were made to fit the elastic hypothesis. Table I lists these values for artificial elastic scattering angles of 90° to 180°. If true inelastic event measurements were fluctuating so as to fit the elastic hypothesis with at least a 2% probability, then they must have $\chi^2<11.6$. Then there would also have to be a pileup of events at $\chi^2$ larger than, but close to 11.6. Table I shows no such pileup. There are various ways of extrapolating the Table I numbers to find how many events might have had $\chi^2<11.6$ and also have had a proton bubble density corresponding to the elastic hypothesis. They all lead to the conclusion that this number is one or less. Since there are eight ambiguous elastic events in this same angular interval the contamination is 12.5% or less. The other angular intervals have smaller contaminations. There were no ambiguities between the elastic hypothesis and the inelastic hypothesis $\pi^-+p\rightarrow\pi^++n+\pi^+$ for barycentric angles beyond 90°. There were a few ambiguous cases of this type for smaller scattering angles, but their effects can be neglected.

TABLE I. $\chi^2$ values of unambiguous inelastic events made to fit the elastic hypothesis and yielding artificial elastic scattering angles of 90° to 180°.

| $\chi^2$ range | Number of events |
|---|---|
| 0 – 11.6 | 0 |
| 11.6– 20 | 0 |
| 20 – 40 | 2 |
| 40 – 60 | 0 |
| 60 – 80 | 1 |
| 80 – 100 | 0 |
| 100 – 200 | 2 |
| 200 – 400 | 3 |
| 400 – 600 | 0 |
| 600 – 800 | 3 |
| 800 –1000 | 2 |
| 1000 –2000 | 17 |
| 2000 –4000 | 16 |
| 4000 –6000 | 13 |
| 6000 –8000 | 14 |

At the beginning of this section it was stated that there is also a difficulty in the bubble chamber analysis of the very small angle region. This difficulty occurs because the scanners have difficulty finding small-angle scatterings with their concomitant short recoil-proton tracks when the plane of the scattering is perpendicular to the chamber window. This effect was seen in this analysis and has been seen elsewhere.[15,16] It is identified by an asymmetric distribution of the scattering plane of small-angle events about the incoming beam axis. Because our interest is primarily in the large angle region, we have not used data at the smaller scattering angles where the required correction was greater than 10%.

Table II presents the corrected elastic scattering data. The cross sections have been corrected for in-

[14] Y. Y. Lee, W. D. C. Moebs, B. P. Roe, D. Sinclair, and J. C. VanderVelde, Phys. Rev. Letters **11**, 508 (1963).

[15] V. Hagopian (private communications).

[16] R. Crittenden, H. J. Martin, W. Kernan, L. Leipuner *et al.*, Phys. Rev. Letters **12**, 504 (1964).

TABLE II. Differential cross sections for 3.63-GeV/$c$ $\pi^-+p$ elastic scattering. Here $\theta^*$ is the pion barycentric scattering angle, $-t$ is the square of the four-momentum transfer in (GeV/$c$)$^2$, and the errors are only statistical.

| Interval in $\cos\theta^*$ | Number of events | $d\sigma/d\Omega$ (mb/sr) | $-t$ at center of interval | $d\sigma/dt$ [mb/(GeV/$c$)$^2$] |
|---|---|---|---|---|
| 0.98 to 0.97 | 298 | 11.1 ±0.6 | 0.0752 | 23.2 ±1.3 |
| 0.97 to 0.96 | 219 | 8.2 ±0.6 | 0.1052 | 17.1 ±1.3 |
| 0.96 to 0.94 | 303 | 5.6 ±0.3 | 0.1503 | 11.7 ±0.6 |
| 0.94 to 0.92 | 205 | 3.8 ±0.3 | 0.210 | 7.9 ±0.6 |
| 0.92 to 0.90 | 118 | 2.20 ±0.20 | 0.271 | 4.6 ±0.4 |
| 0.90 to 0.88 | 85 | 1.58 ±0.17 | 0.331 | 3.3 ±0.4 |
| 0.88 to 0.86 | 44 | 0.82 ±0.13 | 0.391 | 1.71 ±0.27 |
| 0.86 to 0.84 | 24 | 0.45 ±0.09 | 0.451 | 0.94 ±0.19 |
| 0.84 to 0.80 | 26 | 0.24 ±0.05 | 0.541 | 0.50 ±0.10 |
| 0.80 to 0.75 | 16 | 0.12 ±0.03 | 0.676 | 0.25 ±0.06 |
| 0.75 to 0.70 | 6 | 0.045 ±0.018 | 0.827 | 0.094 ±0.038 |
| 0.70 to 0.60 | 18 | 0.064 ±0.015 | 1.052 | 0.134 ±0.031 |
| 0.60 to 0.50 | 16 | 0.057 ±0.014 | 1.353 | 0.119 ±0.029 |
| 0.50 to 0.40 | 11 | 0.039 ±0.012 | 1.653 | 0.081 ±0.025 |
| 0.40 to 0.20 | 6 | 0.011 ±0.004 | 2.10 | 0.023 ±0.008 |
| 0.20 to 0.00 | 2 | 0.0035 ±0.0025 | 2.71 | 0.0073 ±0.0052 |
| 0.00 to −0.20 | 1 | 0.0017 ±0.0017 | 3.31 | 0.0036 ±0.0036 |
| −0.20 to −0.40 | 2 | 0.0033 ±0.0023 | 3.91 | 0.0069 ±0.0048 |
| −0.40 to −0.60 | 1 | 0.0017 ±0.0017 | 4.51 | 0.0036 ±0.0036 |
| −0.60 to −0.80 | 1 | 0.0017 ±0.0017 | 5.11 | 0.0036 ±0.0036 |
| −0.80 to −1.00 | 3 | 0.0050 ±0.0029 | 5.71 | 0.0104 ±0.0061 |

elastic contamination at large angles (a 12.5% or less correction) and for scanning bias at small angles (a 10% or less correction).

A study of the two-prong events which did not fit the elastic or one-pion inelastic hypothesis showed that some elastic events have been lost because of errors in measurement or ionization estimation. No correction has been made for this loss which is less than 10% and is independent of angle.

## III. DISCUSSION

The differential cross section shown in Fig. 1 on a semilogarithmic scale shows the well-known exponential decrease for small values of $-t$. At $\cos\theta^*$ of about +0.60 a secondary peak or at least a plateau can be seen. This is the same kind of structure as was first observed in the 2.0 GeV/$c$ $\pi^-+p$ and $\pi^+ + p$ elastic differential cross section by Damouth, Jones, and Perl.[5] There it appeared as a strong peak at $\cos\theta^*=0.20$ in the $\pi^-+p$ system and at the same $\cos\theta^*$, but weaker, in the $\pi^+ + p$ system. Since then, Hagopian has found this second peak clearly in 3.0 GeV/$c$ $\pi^-+p$ elastic scattering at $\cos\theta^*=0.52$. Weak evidence of it also appears in the 4.0 GeV/$c$ $\pi^-+p$ system[6] at $\cos\theta^*=0.65$. Simmons[17] first explained the second peak at 2.0 GeV/$c$ as a second diffraction maximum and considered it unrelated to any $\pi+p$ resonances. Perl and Corey[9] continued this interpretation. Most of the evidence for this second peak is in the $\pi^-+p$ system, but this may be due to the relative scarcity of $\pi^+ + p$ data with high statistics. For the present, the simplest assumption is that the second diffraction maximum occurs in both $\pi+p$ systems. Table III lists the position of this maximum. It is very impressive that the position is independent of the incident momenta when expressed in terms of $t$. In fact, we have even included the large backward peaks found in the $\pi^+ + p$ system[18] at 1.5 GeV/$c$ and in the $\pi^-+p$ system[19–21] at 1.5 and 1.59 GeV/$c$ without the $t$ position

[17] L. M. Simmons, Phys. Rev. Letters **12**, 229 (1964).

TABLE III. Position of secondary diffraction maximum in various $\pi+p$ systems.

| System | Position $\cos\theta^*$ | $-t$ [(GeV/$c$)$^2$] | Reference |
|---|---|---|---|
| 2.01-GeV/$c$ $\pi^-+p$ | 0.20 | 1.20 | a |
| 2.02-GeV/$c$ $\pi^+ + p$ | 0.20 | 1.20 | a |
| 3.0-GeV/$c$ $\pi^-+p$ | 0.52 | 1.17 | b |
| 3.63-GeV/$c$ $\pi^-+p$ | 0.60 | 1.20 | |
| 4.0-GeV/$c$ $\pi^-+p$ | 0.65 | 1.17 | c |
| 1.5-GeV/$c$ $\pi^+ + p$ | −0.35 | 1.43 | d |
| 1.59-GeV/$c$ $\pi^-+p$ | −0.15 | 1.40 | e |
| 1.5-GeV/$c$ $\pi^-+p$ | −0.40 | 1.48 | f, g |

[a] D. E. Damouth, L. W. Jones, and M. L. Perl, Phys. Rev. Letters **11**, 287 (1963).
[b] V. Hagopian (private communications).
[c] M. Aderholz, L. Bondar, M. Deutschmann, H. Lengeler *et al.*, Phys. Letters **10**, 245 (1964); Nuovo Cimento **31**, 729 (1964).
[d] V. Cook, B. Cork, W. Holly, and M. L. Perl, Phys. Rev. **130**, 762 (1963).
[e] J. Alitte, J. P. Barton, and A. Berthelot, Nuovo Cimento **29**, 515 (1963).
[f] M. Chretien, J. Leitner, N. P. Samios, M. Schwartz, and J. Steinberger, Phys. Rev. **108**, 383 (1957).
[g] K. W. Lai, L. W. Jones, and M. L. Perl, Phys. Rev. Letters **1**, 125 (1961).

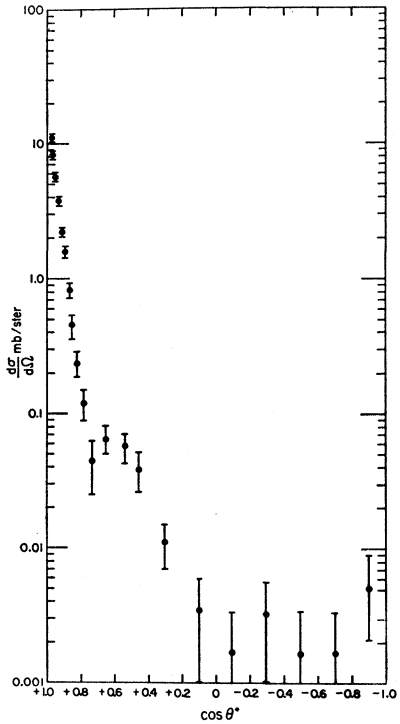


FIG. 1. A semilogarithmic plot of the elastic differential cross section of 3.63-GeV/$c$ $\pi^-$ mesons on protons. The cross section is in units of mb/sr, and $\cos\theta^*$ is the cosine of the barycentric scattering angle of the $\pi^-$. The error bars give the statistical error.

[18] V. Cook, B. Cork, W. Holly, and M. L. Perl, Phys. Rev. **130**, 762 (1963).
[19] M. Chretien, J. Leitner, N. P. Samios, M. Schwartz, and J. Steinberger, Phys. Rev. **108**, 383 (1957).
[20] J. Alitte, J. P. Barton, and A. Berthelot, Nuovo Cimento **29**, 515 (1963).
[21] K. W. Lai, L. W. Jones, and M. L. Perl, Phys. Rev. Letters **1**, 125 (1961).

TABLE IV. Average differential cross section for $0.0 \geq \cos\theta^* \geq -1.0$ in $\pi^- + p$ elastic scattering.

| Incident momentum (GeV/$c$) | $d\sigma/d\Omega$ ($\mu$b/sr) | $d\sigma/dt$ [$\mu$b/(GeV/$c$)$^2$] | Reference |
|---|---|---|---|
| 3.0 | 4.0± 1.0 | 10.0± 2.0 | a |
| 3.63 | 2.7± 1.0 | 5.4± 2.0 | |
| 4.0 | 12.0±12.0 | 23.0±23.0 | b |

[a] V. Hagopian (private communications).
[b] M. Aderholz, L. Bondar, M. Deutschmann, H. Lengeler *et al.*, Phys. Letters **10**, 245 (1964); Nuovo Cimento **31**, 729 (1964).

changing greatly. Thus good evidence is emerging that this second diffraction maximum is almost independent in position of the incident momentum. However, as the incident momentum increases, its relative magnitude decreases.

Returning to Fig. 1, we observe that for $0.0 > \cos\theta^* > -1.0$, the differential cross section is flat within statistics, although a rise at $\cos\theta^* = -1.0$ may exist. The average differential cross section in this angular range is $2.7 \pm 1.0$ $\mu$b/sr. Table IV compares this measurement with other measurements of the average backward differential cross section in the $\pi^- + p$ systems. The 3.63-GeV/$c$ measurement is in good agreement with the 3.0 and 4.0 measurement. Unfortunately there are no published measurements at higher incident momenta which can be used to establish the rate of decrease of the scattering back of 90°. At lower momenta, much below 3.0 GeV/$c$, the backward differential cross section is definitely not flat. For example, at 2.0 GeV/$c$ the cross section decreases by a factor of 10 from $\cos\theta^* = 0.0$ to $\cos\theta^* = -0.80$ and then seems to rise again as $\cos\theta^*$ approaches $-1.0$. The average value is $51 \pm 3$ $\mu$b/sr, but it is certainly not meaningful to compare this number with the numbers of Table IV which seem to represent a roughly flat cross section.

To compare these data with the large-angle behavior of $p+p$ elastic scattering, we have constructed Table V. The $p+p$ data are taken from a graph in a report of the recent measurements of Clyde and his colleagues.[22] At these incident momenta the masses of the particles are still important, and it is not clear what incident momenta $p+p$ system should be compared with a particular incident momenta $\pi^- + p$ system. Therefore, we have also listed the kinetic energy $T^*$ available in the barycentric system, and $s$ the square of the total energy in the barycentric system. The $p+p$ differential cross sections are the 90° points, while the $\pi^- + p$ differential cross sections are the average from 90 to 180°.

TABLE V. Comparison of $p+p$ and $\pi^- + p$ large-angle elastic scattering.

| System | Incident momenta (GeV/$c$) | $T^*$ (GeV) | $S$ [(GeV)$^2$] | $-t$ position or range [(GeV/$c$)$^2$] | $d\sigma/dt$ [$\mu$b/(GeV/$c$)$^2$] |
|---|---|---|---|---|---|
| $p+p$ | 3.0 | 1.0 | 7.7 | 2.1 | 650.0±50.0 |
| $p+p$ | 5.0 | 1.6 | 11.3 | 3.9 | 20.0± 5.0 |
| $p+p$ | 7.1 | 2.1 | 15.2 | 5.8 | 0.8± 0.2 |
| $\pi^- + p$ | 3.0 | 1.6 | 6.5 | 2.4 to 4.8 | 10.0± 2.0 |
| $\pi^- + p$ | 3.63 | 1.8 | 7.7 | 3.0 to 6.0 | 5.4± 2.0 |

[22] A. R. Clyde, B. Cork, D. Keefe, L. T. Keith, W. M. Layson, and W. A. Wenzel, University of California Radiation Laboratory Report No. UCRL 11441 (unpublished).

If the same $s$ is used for comparison, then the 3.0 and 3.63 GeV/$c$ $\pi^- + p$ cross sections are much smaller than the comparable-$s$ $p+p$ cross section at 3.0 GeV/$c$. If the same $T^*$ is used for comparison, then the 3.0 GeV/$c$ $\pi^- + p$ cross section should be compared to the 5.0 GeV/$c$ $p+p$. Here also the $t$ range of the $\pi^- + p$ spans the $p+p$ 90° $t$ values. The $\pi^- + p$ cross section is just half that of the $p+p$. But the $p+p$ differential cross section keeps decreasing rapidly from 5.0 to 7.1 GeV/$c$, while the 3.63-GeV/$c$ $\pi^- + p$ measurement indicates that the $\pi^- + p$ seems to be dropping much more slowly. Therefore, it seems possible that above this energy range the $p+p$ large-angle cross section is considerably less than the $\pi^- + p$ cross section. However, the errors of the $\pi^- + p$ values are large, and it is still possible that the $\pi^- + p$ is decreasing as rapidly as the $p+p$.

The peak in $\pi^+ + p$ elastic scattering at 180° recently found at 4.0 GeV/$c$ has[6] been predicted for some time on the basis of a virtual neutron exchange model. But there is no basic theoretical calculation for this phenomenon, and the explanation of the backward peak is

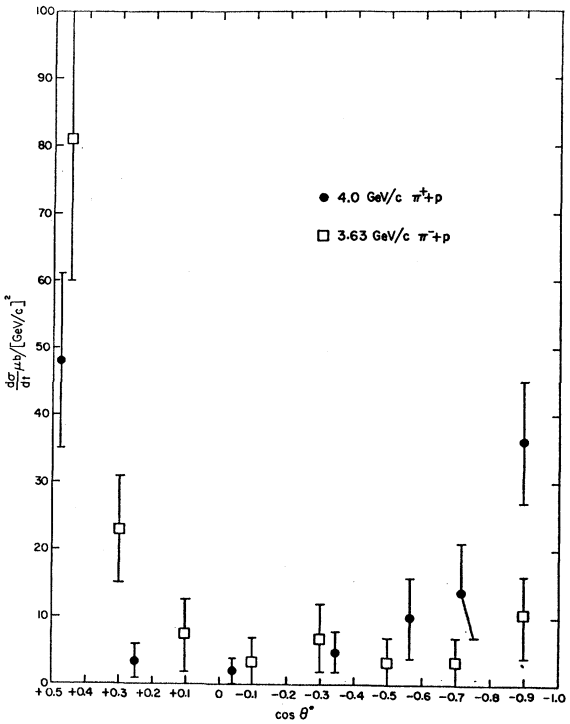


FIG. 2. Comparison of large-angle elastic scattering of 4.0-GeV/$c$ (solid circles) $\pi^+ + p$ and 3.63-GeV/$c$ (open squares) $\pi^- + p$. The differential cross section is in units of microbarns per steradian and is plotted versus $\cos\theta^*$ where $\theta^*$ is the barycentric scattering angle of the $\pi$. The error bars give the statistical errors.

TABLE VI. Values of $(1-a_l)$ for the 3.63-GeV/$c$ $\pi^-+p$ and 4.0-GeV/$c$ $\pi^+ + p$ systems.

| System | $\pi^-+p$ | | $\pi^+ + p$ | | $\pi^+ + p$ | |
|---|---|---|---|---|---|---|
| Incident lab momentum (GeV/$c$) | 3.63 | | 4.00 | | 4.00 | |
| | | | | | With backward peak removed | |
| Max $l$ | 9 | 10 | 9 | 10 | 9 | 10 |
| $1-a_0$ | 1.00 ±0.05 | 1.01 ±0.05 | 1.000±0.001 | 1.000 ±0.001 | 1.000±0.001 | 1.000 ±0.001 |
| $1-a_1$ | 0.70 ±0.05 | 0.70 ±0.05 | 0.877±0.025 | 0.876 ±0.025 | 0.880±0.024 | 0.878 ±0.024 |
| $1-a_2$ | 0.525±0.048 | 0.531 ±0.049 | 0.566±0.022 | 0.557 ±0.022 | 0.582±0.021 | 0.584 ±0.021 |
| $1-a_3$ | 0.383±0.049 | 0.376 ±0.050 | 0.548±0.022 | 0.547 ±0.022 | 0.500±0.021 | 0.498 ±0.021 |
| $1-a_4$ | 0.270±0.047 | 0.276 ±0.048 | 0.197±0.020 | 0.198 ±0.020 | 0.252±0.018 | 0.253 ±0.018 |
| $1-a_5$ | 0.211±0.046 | 0.206 ±0.046 | 0.312±0.020 | 0.311 ±0.020 | 0.258±0.017 | 0.257 ±0.017 |
| $1-a_6$ | 0.137±0.040 | 0.143 ±0.040 | 0.060±0.017 | 0.060 ±0.017 | 0.108±0.015 | 0.109 ±0.015 |
| $1-a_7$ | 0.095±0.033 | 0.091 ±0.034 | 0.168±0.014 | 0.168 ±0.014 | 0.127±0.013 | 0.126 ±0.013 |
| $1-a_8$ | 0.032±0.023 | 0.035 ±0.024 | 0.001±0.009 | 0.002 ±0.009 | 0.029±0.009 | 0.029 ±0.009 |
| $1-a_9$ | 0.014±0.015 | 0.013 ±0.015 | 0.053±0.008 | 0.053 ±0.008 | 0.037±0.008 | 0.036 ±0.008 |
| $1-a_{10}$ | | 0.0010±0.0010 | | 0.0005±0.001 | | 0.0008±0.001 |

still really obscure.[4,18] Our 3.63-GeV/$c$ $\pi^-+p$ data show that no such large backward peak exists in the $\pi^-+p$ system in this incident momentum range. A direct comparison of the two systems is made in Fig. 2. As $\cos\theta^*$ approaches 0 both cross sections decreased in a quantitatively similar way. From $+0.1$ to $-0.5$ both cross sections are flat and have the same value within the statistical errors. But then the $\pi^+ + p$ system rises to $36\pm9\,\mu\text{b}/(\text{GeV}/c)^2$ whereas the $\pi^-+p$ rises to $10\pm6\,\mu\text{b}/(\text{GeV}/c)^2$. If the incident momentum difference can be neglected, then it is clear that the $\pi^+ + p$ differential cross section has a backward peak about 3 or 4 times as large as the backward $\pi^-+p$ differential cross section.

Perl and Corey[9] have made an analysis of $\pi+p$ differential cross sections with the partial wave equation

$$\frac{d\sigma}{d\Omega}=\left|\frac{1}{2k}\sum_{l=0}^{l_{\max}}(2l+1)(1-a_l)P_l(\cos\theta^*)\right|^2,$$

where $k$ is the wave number in cm$^{-1}$ of the particles in the barycentric system, $\theta^*$ is the scattering angle in that system, and $P_l$ is the Legendre polynomial of order $l$. If we require that $a_l$ be real and that $1\geq(1-a_l)\geq0$, then we are using a purely absorptive model of elastic scattering. This model also sets the spin-flip amplitudes to zero.

With the aforementioned constraint on $(1-a_l)$, a weighted least-square fit was made to the 3.63 GeV/$c$ $\pi^-+p$ and 4.0-GeV/$c$ $\pi^+ + p$ data to determine the $(1-a_l)$ values. To see the effect of the backward peak, we have also made a fit to the 4.0 $\pi^+ + p$ data in which the backward peak was removed and the $\pi^+ + p$ differential cross section was taken as flat from 90 to 180° using its 90° value. To decide what $l_{\max}$ to use, repeated fits were made for increasing values of $l_{\max}$ until there was no longer a substantial change in the $(1-a_l)$ values obtained. This occurred when $l_{\max}$ went from 9 to 10, and these are the values of $l_{\max}$ used in Table VI. The difference between the $\pi^+ + p$ data with the backward peak, on one hand, and the $\pi^+ + p$ data without the backward peak and the $\pi^-+p$ data, on the other hand, is clear. The latter systems have an almost monotonically decreasing set of $(1-a_l)$ values. The former has an alternating set of $(1-a_l)$ magnitudes for the larger $l$ values. Thus, $(1-a_4)$, $(1-a_6)$, and $(1-a_8)$ are relatively smaller while $(1-a_5)$, $(1-a_7)$, and $(1-a_9)$ are relatively larger. This is an obvious way for a backward peak to build. If the $(1-a_l)$ values decrease smoothly and monotonically, then the partial wave amplitudes almost completely cancel at 180°. But if alternate ones are larger there is less cancellation. This is not a basic explanation of the backward peak, but it does show that it cannot be ascribed to a particular $l$ value.

## ACKNOWLEDGMENTS

We are grateful for the assistance of the Shutt Bubble Chamber Group and the AGS staff at the Brookhaven National Laboratory. We also thank Professor B. P. Roe, Professor D. Sinclair, and Professor J. C. VanderVelde for their help during the early stages of the experiment.